Geophysical and geotechnical characterization of small earth dams in the Piedmont region for seismic risk assessment

Renato Maria Cosentini
Department of Structural, Building and Geotechnical Engineering, Politecnico di Torino, Turin, Italy,
renato.cosentini@polito.it

Sebastiano Foti, Federico Passeri
Department of Structural, Building and Geotechnical Engineering, Politecnico di Torino, Turin, Italy,
sebastiano.foti@polito.it, federico.passeri@hotmail.it

ABSTRACT: Earth dams are defined "small" when their height is up to 15 m and their reservoir volume is lower than 10^6 m^3. Despite the small cubage of the reservoir volume, the risk associated with their potential rupture can be considerable. Indeed, they are often located along slopes close to populated areas and they are characterized by lack of technical information. The main goal of the "ReSba" project is to improve the knowledge regarding the risks of dams and the resilience of the community. This project, sponsored by the European fund for regional development (Interreg-ALCOTRA) for the French-Italian Alps, involved about 100 earth dams in the Piedmont region (Italy). In this respect, a geophysical and geotechnical characterization campaign has been set up to for few of these small earth dams. The geophysical tests were primarily based on surface wave methods and down-hole invasive tests. The geotechnical investigations included static and dynamic laboratory tests conducted on undisturbed samples. The selection criterion of the dams to be investigated was based on a simplified procedure for the evaluation of the seismic risk associated with the dam. The results of these tests are finalized to assess the seismic risk of the dam through both simplified pseudo-empirical methods and advanced numerical dynamic analyses.

Keywords: Earth dam; Seismic risk; Seismic vulnerability, Geophysical investigation, Laboratory investigation

1. Introduction

The Italian National Technical Code for Dams [1] dedicates a specific section to the assessment of seismic safety of existing dams. Following the Italian Technical Code [2], seismic risk studies are based on the concept of "gradualness", i.e. the assessment of seismic risk can be performed adopting models of increasing complexity according to the level and quality of available information. In this respect, it is possible to adopt complex models of analysis only for "large dams". Indeed in these cases a large number of high quality information is typically available. "Large dams" are characterized by a height over 15 m or/and a reservoir volume higher than 10^6 m^3 [1]. In Italy, there are about 530 large dams, 165 of them are earth dams [3]. Most of them were built before of shortly after the middle of the last century, therefore data and information about their design, building and monitoring are considerable [4]. Such information allows a complete characterization of the structure and seismic safety analyses through advanced dynamic methods.

On the contrary, the technical information and data for "small dams", characterized by a height up to 15 m and a reservoir volume lower than 10^6 m^3 [1], are lacking. The last survey carried out by ISPRA (Italian Institute for Environmental Protection and Research) shows that in Italy there are more than 10000 small dams [5]. About 700 are located in the Piedmont region; approximatively 100 of them are small earth dams located close to populated areas of the Alps region (Fig. 1). Therefore, the risk associated with their potential rupture can be considerable in spite of the small cubage of their reservoir volume. Moreover, many of these dams generally were built with limited economical resources and therefore with simple technologies, compacting local natural materials. Hence, the evaluation of seismic vulnerability of these types of dams is of paramount importance for Civil Protection purpose.

In this respect, the "ReSba" (Resilienza degli Sbarramenti) project aims to improve the knowledge regarding the risk associated to these dams and the related resilience of the community. It is a project funded by the European Union for regional development (Interreg-ALCOTRA) for the French-Italy Alps. In the project a very simple methodology has been adopted to systematically classify the small earth dams located in French-Italy boundary area in terms of their associated seismic risk.

On the basis of this preliminary study, four small earth dams have been selected for a geotechnical and geophysical characterization campaign: the first located within the municipality of Arignano (TO), two within the municipality of Envie (CN) ("La Grengia" dams, "Cascina Rubiolo " dams), and the last in Briaglia (CN).

Geophysical tests have been mainly based on active multi-channel analysis of surface waves (MASW) tests, ambient vibration surveys (including 2D array measurements and single-station Horizontal to Vertical Spectral Ratio - HVSR), down-hole tests, and 1D electric resistivity tomography.

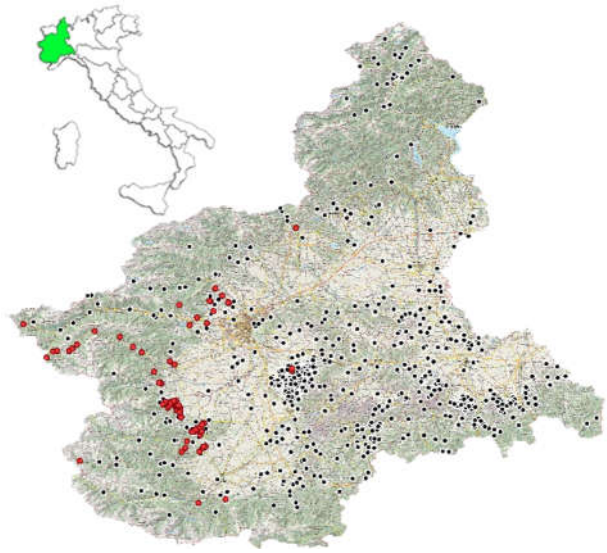

Figure 1. Localization of Piedmont region dams (black and red dots). Red dots are earth dams included in ReSba project.

In situ geotechnical investigation included: cone penetration tests with acquisition of the excess pore water pressure, and compressional and shear wave velocity (SCPTu), flat dilatometer test (DMT), and drilling of boreholes.

Static and dynamic laboratory tests have been also performed on undisturbed soil samples retrieved from boreholes.

The dataset of this campaign can be gathered with the scope to build a numerical model on which advanced dynamic analyses can be performed to assess the seismic vulnerability of each dam.

2. Preliminary seismic risk assessment of Piedmont small earth dams

The seismic risk assessment of a great number of structure is not easy activity, especially when the technical information are lacking. Actually, no advanced approach can be used in these cases.

To overcame this limitation and to define a preliminary criterion to identify the most critical structures that need a priority in planning further investigations and analyses, a very simplified procedure to evaluate the seismic risk of small earth dams has been recently proposed [6]. The methodology is based on the compilation of datasheets that lead to a preliminary classification of earth dams in terms of their associated seismic risk.

Specifically, the three factors that define seismic risk (H: hazard; E: exposure; V: vulnerability) are combined following a Multi Criteria Decision Making (MCDM) protocol to evaluate an representative index of the seismic risk for small earth dams (Tab.1).

The hazard factor (H) is computed as

$$H = (4 - Z) + 1 \quad (1)$$

where Z is an integer number that represents the seismic zone in which the earth small dam falls. Indeed, since 2003 the Italian territory has been classified in four seismic categories, according to the maximum outcrop acceleration (PGA) with a probability of exceedance equal to 10% in 50 years: zone 1 PGA=0.35g; zone 2 PGA=0.25g; zone 3 PGA=0.15g; zone 4 PGA=0.05g. Intermediate classes were added in 2015 when an update of this classification was released. The seismic zonation map of Piedmont region is shown in Fig. 2.

The exposure (E) is defined using a simplified study of break-dam scenarios performed by Piedmont regional administration [7]. Three levels of exposure are defined (Tab. 2).

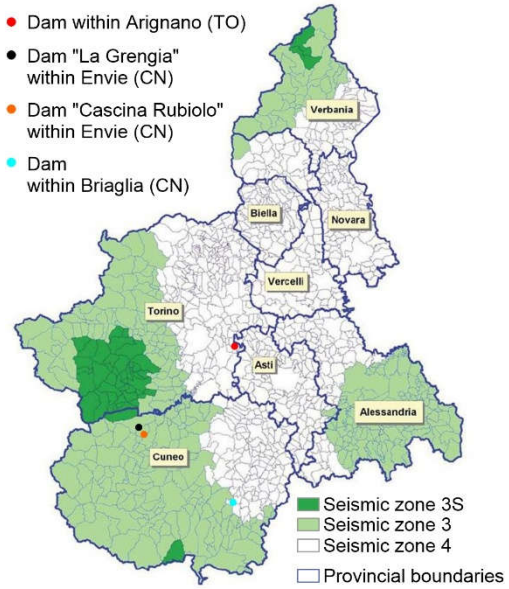

Figure 2. Piedmont region seismic zonation map with location of the four dams selected for geotechnical and geophysics characterization campaign in the ReSba project.

Table 1. Matrix to evaluate seismic risk

	Vulnerability	Maximum			High			Moderate			Low			Negligible		
	Exposure	High	Medium	Low	High	Medium	Low	High	Medium	Low	High	Medium	Low	High	Medium	Low
Hazard	Zone 1	17	16	15	14	13	12	11	10	9	8	7	6	5	4	3
	Zone 2	16	15	14	13	12	11	10	9	8	7	6	5	4	3	2
	Zone 3	15	14	13	12	11	10	9	8	7	6	5	4	3	2	1
	Zone 4	14	13	12	11	10	9	8	7	6	5	4	3	2	1	0

Table 2. Exposure values

Classes of exposure		**E**
Low	Negligible economic and environmental losses in downstream areas	1
Medium	Serious environmental consequences or significant economic losses and damage of commercial and/or industrial facilities, public services and/or structure in downstream areas (unlikely loss of life)	2
High	Losses of life and significant economic damage in downstream areas (urban areas with several inhabitants)	3

Finally, the vulnerability factor (V) is computed though an index (V_{st}) defined as the sum of four parameters (Eq. 2) for the limit state corresponding to a 10% exceedance probability in 50 years [2]:

$$V_{st} = V_{cond} + V_{liq} + V_{sett} + V_{disp} \quad (2)$$

where:

- V_{cond} is the vulnerability of the dam due to its general state. It is defined through a direct in situ inspection. This parameter varies between 0.2 and 1, and it increases as the deterioration phenomena affecting the body of dam are more evident.
- V_{liq} is the vulnerability due to liquefaction phenomena. The value of this parameter is 0 if one of the exclusion criteria proposed by NTC [2] is satisfied, and 1 in other cases or in absence of direct observations.
- V_{sett} is the vulnerability due to the potential crest settlements. This parameter is defined as the ratio between the expected settlement and a threshold value of 0.02%, corresponding to a moderate levels of damage [8]. The expected settlement w is evaluated through the relationship proposed by Swaisgood [8]:

$$w(\%) = e^{(6.07 \cdot PGA + 0.57 \cdot M - 8)} \quad (3)$$

  where M is the earthquake magnitude and PGA (in g) is the Peak Ground Acceleration.
- V_{disp} is the vulnerability due to expected slope displacements along the side of the dam. Also this parameter is defined as the ratio between the predicted slope displacements and a reference value. The predicted slope displacement can be computed following an empirical formulation, like the one proposed by Blake et al. [9]:

$$u_d(mm) = k_{max} \cdot D_{5-95} \cdot 10^{1.87 - 3.477 \frac{k_y}{k_{max}}} \quad (4)$$

  where $D_{5\text{-}95}$ is the significant duration of shaking in seconds (i.e. the time interval between 9-95% of the normalized Arias intensity), $k_{max} = PGA/g$ (where g is gravity acceleration), and k_y is the yield acceleration of the slope (i.e. the horizontal seismic coefficient that reduces the factor of safety for the slope to unity). This last parameter can be preliminarily estimated on the basis of the static factor of safety (FS) as: $k_y = (FS\text{-}1) \cdot \sin \alpha$, where α is the average angle of the failure surface with the horizontal. In the proposed methodology $k_y = 0$ is assumed if no specific slope stability analyses are available. Following the study of Blake et al. [9], a value of 5 cm was assumed for the threshold values of the slope displacements.

On the basis of this approach five classes of seismic risk have been defined (Tab.3)

The four small earth dams selected for the geotechnical and geophysics characterization campaign described in details below were classified from medium to high risk, according the proposed approach.

Table 3. Scale of seismic risk index

Range of index	**Class of risk**	
0 ÷ 4	A	Low
5 ÷ 7	B	Low – medium
8 ÷ 10	C	Medium
11 ÷ 13	D	Medium – High
14 ÷ 17	E	High

3. Ground characterization campaign

The aim of ground characterization campaign was to increase the technical knowledge on the selected earth dams and to define the geotechnical ground model needed to perform seismic risk assessment through advanced methods.

Table 4. Type of in-situ tests for each investigated dam

Dams	**Tests**
Arignano (TO)	Geophysical tests: • MASW and 2D AVA • HVSR • ERT
	Geotechnical tests • SCPTU • DMT
Envie (CN) "La Grengia"	Geophysical tests: • MASW • DH
	Geotechnical tests • Borehole (with sampling) • SCPTU • DMT
Envie (CN) "Cascina Buglione"	Geophysical tests: • DH
	Geotechnical tests • Borehole (with sampling) • SCPTU • DMT
Briaglia (CN)	Geophysical tests: • MASW • HVSR • DH
	Geotechnical tests • Borehole (with sampling) • SCPTU • DMT
MASW – Active multi-channel analysis of surface wave tests; 2D AVA – Passive Ambient Vibration 2D Array test; HVSR – Horizontal to Vertical Spectral Ratio test; DH – Down-hole test; ERT: Electric Resistivity Tomography test; SCPTU- Seismic Cone Penetration Test with measure of pore pressure; DMT-Flat Dilatometer Test.	

In this respect geotechnical and geophysical in situ tests were carried out. The details of the tests for each dam is reported in Tab. 4. The amount and type of investigation have been selected taking into account available information for each dam.

During boreholes same undisturbed samples were collected. Static and dynamic laboratory tests were performed on these samples, as well.

In this paper the results obtained at the dam located within the municipality of Briaglia (CN) are presented.

3.1. Briaglia dam

The dam is located within the municipality of Briaglia (CN) (Fig. 3) and it was built at the beginning of 1990s.

Figure 3. Location and representative pictures of Briaglia dam.

It is a typical trapezoidal shape homogeneous embankment (Fig. 4) with a spillway and adequate rockfill on the upstream to protect the dam from the wave flux.

The main physical and geometric characteristic of the dam are reported in Tab. 5.

Table 5. Characteristics of Briaglia dam

Parameter	Value
Height	10.83 m
Reservoir volume	59500 m^3
Elevation of top of dam.	455.30 m sl
Elevation of Flashboards	155.30 m sl
Crest length	88.50 m
Crest width	4.00 m

3.1.1. In situ geotechnical tests

To define the soil profile of the body of the dam and the soil foundation, a borehole was drilled, from the dam crest up to a maximum depth of 30 m. The relative soil profile is sketched in Fig. 4.

The soil profile is composed of:

- 0.20 m of organic soil (crest of dam);
- 4.30 m of medium-dense sandy silt (body of dam);
- 1.30 m of medium stiff clayey silt (body of dam);
- 0.80 m of mixed soil composed of arenites and marly (body of dam);
- 6.40 m of low to medium dense silty-clayey sand, with some arenites having sometimes block dimension (body of dam/foundation);
- 6.00 m of medium stiff clay with local laminae of arenites having a thickness of 30 – 50 cm (foundation);
- 10.00 m of low stiff clayey marl with some local laminae of arenites having a thickness of 30 – 50 cm (foundation).

During drilling, three undisturbed soil samples were retrieved with the standard Osterberg sampler. The first sample was collected at 3.00m depth, the second at 15.00m and the last at 27.50m.

At the end of the drilling, the borehole was equipped with a PVC pipe casing to perform down-hole tests.

Other two in-situ tests were performed near the borehole. The first test is a cone penetration tests with acquisition of the pore water pressure and measurement of the compressional and shear wave velocities (SCPTU). Unfortunately, the test was stopped after about 6 m from the top of the dam probably because the very stiff layer composed of arenites and marly was met. The results obtained from this test are reported in Fig. 5.

The second test is a flat dilatometer test (DMT). Measures performed every 20 cm and the obtained parameters are reported in Fig.6. The test was stopped at the depth of about 16 m because the capacity of the contrast mass was reached.

3.1.2. In situ geophysical tests

Invasive and non-invasive geophysical tests were performed to characterize the body and the foundations of dam.

In particular, a Down-hole test, a set of Multi-channel analysis surface wave tests (MASW), and a horizontal to vertical spectral ratio survey (HVSR) were carried out.

The Down-hole test was executed by means of a seismic chain of 8 triaxial geophones (10 Hz) with 1 m spacing. Data were acquired with a Geomatrix - Geode seismograph. The seismic chain was lowered into the hole with a 2 geophones superposition for consecutive lowering. For P waves a 8 kg sledge-hammer striking vertically on a steel plate was used; for S waves the same hammer striking laterally on a 1.5 m steel bar was adopted. Polarity inversion was used for S waves acquisition. Data was processed, after first break picking, both with the interpolation method and with the true interval method. The results obtained from the Down-hole test is here shown only in terms of shear wave velocity (Fig. 7).

Surface wave tests (MASW – Multichannel Analysis of Surface Waves) were performed following the Guidelines of the Interpacific project [10]. A first survey was performed using an array of 48 vertical geophones with a total length of 70,5 m, disposed along the top of dam. The seismic source was a 5 kg sledge hammer striking vertically on a steel plate. Shot offsets were +2 and +4 m on both sides of the seismic line.

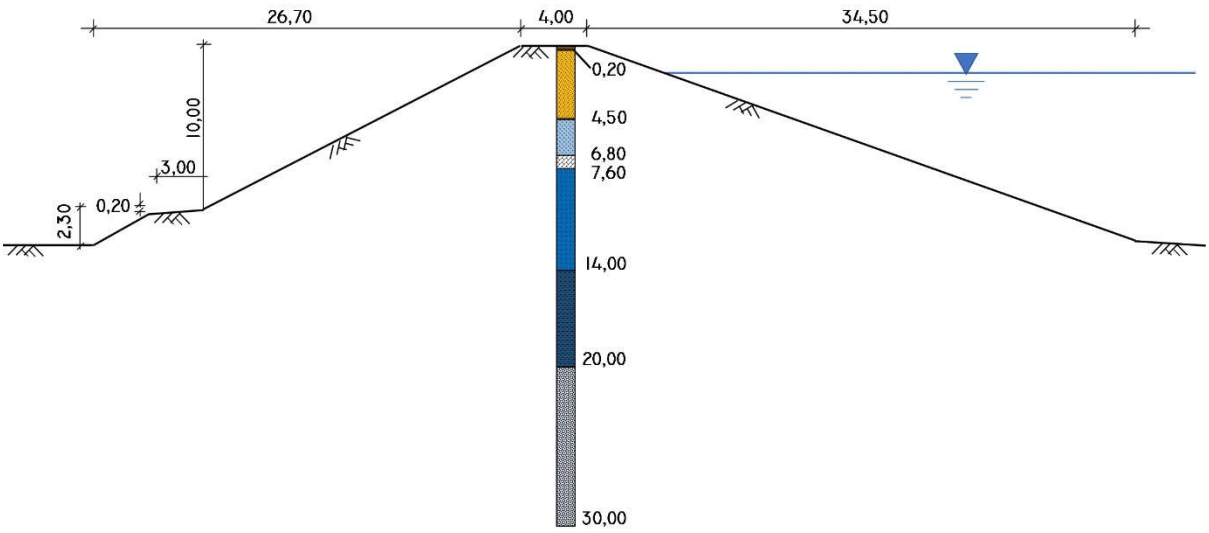

Figure 4. Main cross section of Briaglia dam with the sketch of soil profile .

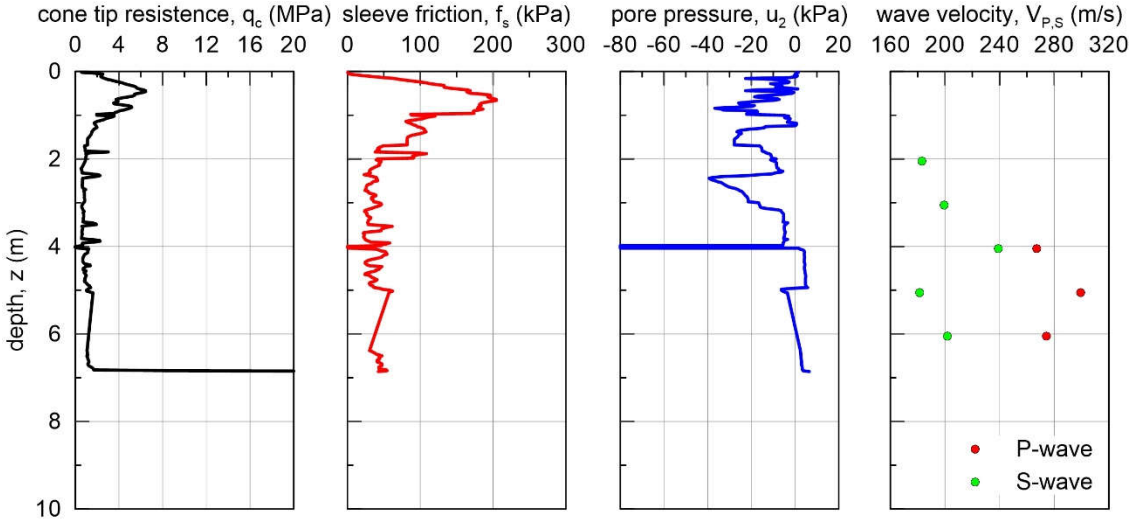

Figure 5. SCPTU test results: cone tip resistance, sleeve friction, pore pressure, and P/S - wave velocity versus depth.

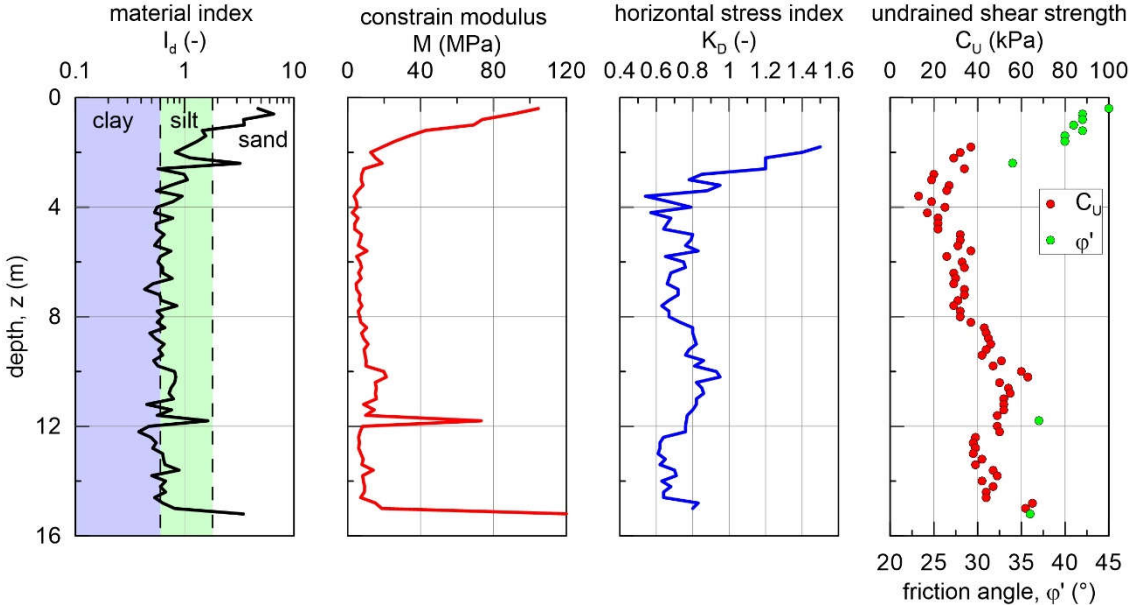

Figure 6. DMT test results: material index, constrain modulus, horizontal stress index, undrained shear strength, and friction angle versus depth.

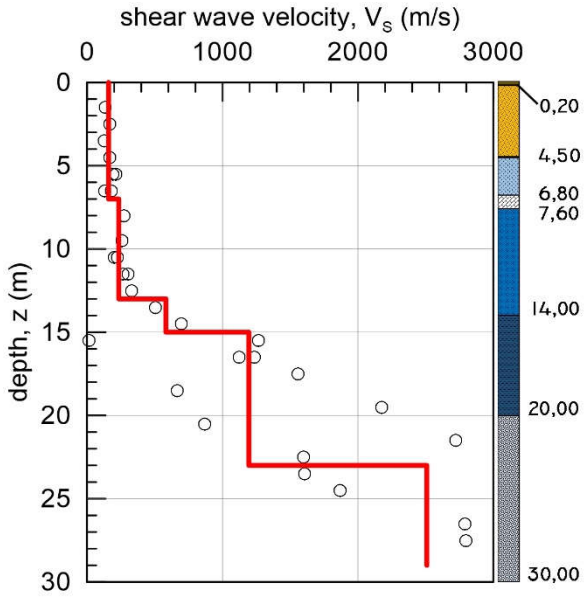

Figure 7. Down-Hole test results.

Different shots from both the directions were repeated and stacked during the processing of the acquired data.

A second surface wave test was executed placing 27 vertical geophones with 1 m spacing on the area at the toe of dam parallel to it. In this case shot offsets were +1 and +2 m on both sides of the seismic line.

Data were processed in the f–k domain with the Surface Wave Analysis Tool (SWAT) code developed in MATLAB environment at Politecnico di Torino, for dispersion curve estimation. These curves were inverted, with a Monte Carlo Inversion algorithm [11].

Figs. 8 and 9 show the Experimental Dispersion Curve (black dots with their standard deviation) with the set of best fitting Theoretical Dispersion Curves for the top of dam and toe of embankment, respectively. Red lines represent theoretical dispersion curves with minimum misfit.

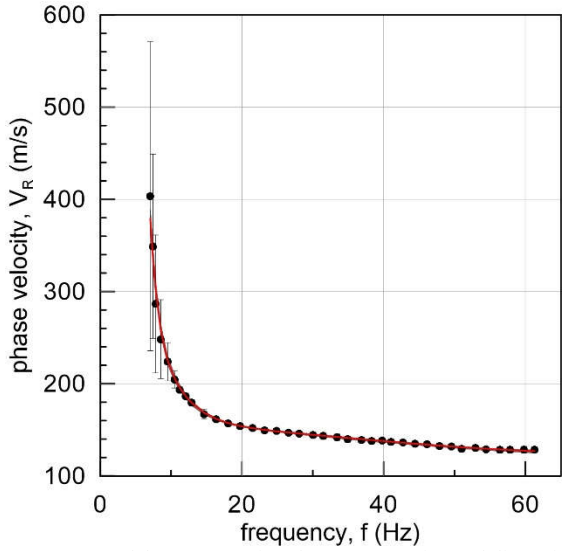

Figure 8. Top of dam - comparison between experimental dispersion curve (black dots with their standard deviation) and best fitting theoretical dispersion curves. The red line is the theoretical dispersion curve with the minimum misfit.

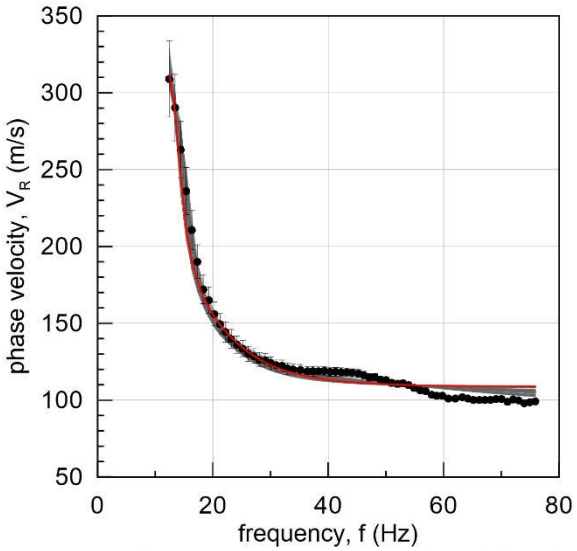

Figure 9. Toe of dam - comparison between experimental dispersion curve (black dots with their standard deviation) and about 80 theoretical dispersion curves. The red line is the theoretical dispersion curve with minimum misfit.

Results of inversion process are shown for both tests in Figs. 10 and 11 as interval velocity profiles (on the left) and corresponding harmonic average shear wave velocity profile (on the right). In both figures red line represents the minimum misfit profile.

Finally, a Horizontal to Vertical Spectral Ratio test (HVSR) was performed with a single 3-component receiver at the crest of dam. The recording time was set following the standard proposed in SESAME project [12].

Data were processed breaking recording of each component into time steady-state windows and transform them into frequency domain using a Discrete Fourier Transform. For each windows horizontal components were combined before to evaluate the experimental H/V ratio curve. The obtained mean H/V curve (continuous line) with standard deviation (dash lines) are shown in Fig. 12. The shaded area represents the frequency range where the curve shows a peak.

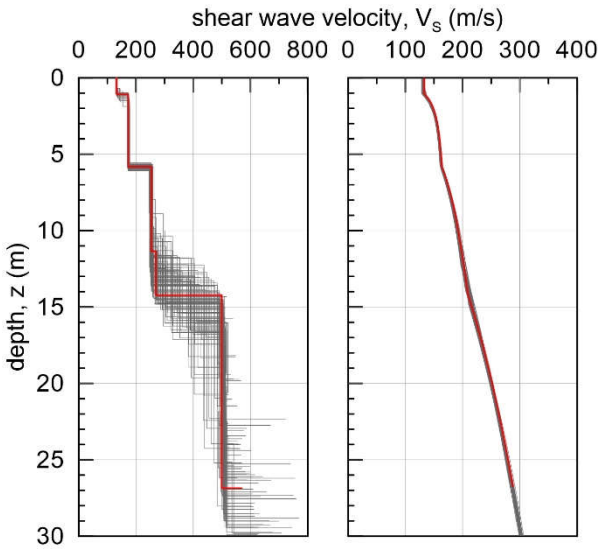

Figure 10. Top of dam - Statistical sample of the interval velocity shear profile (on the left), and statistical sample of the harmonic average shear wave velocity profiles (on the right).

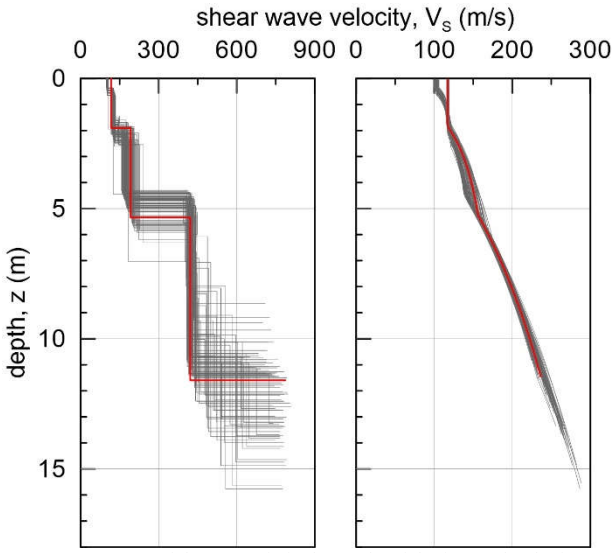

Figure 11. Top of dam - Statistical sample of the interval velocity shear profile (on the left), and statistical sample of the harmonic average shear wave velocity profiles (on the right).

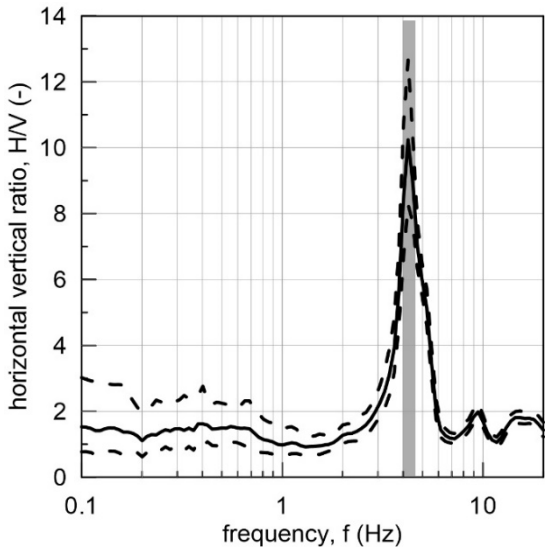

Figure 12. H/V curve with identification of main site fundamental resonant frequency.

3.1.3. Laboratory tests

Undisturbed samples retrieved from the borehole were tested in the laboratory to determine physical and mechanical properties of dam and foundation soils.

The laboratory program is reported in Tab. 6.

In the following the results of each test are illustrated and discussed.

Table 7 reports a summary of main physical and state variables obtained on samples subjected to static or cyclic/dynamic tests.

Grain size distributions reported in Fig. 13, shows that the dam crest is mainly composed of silt with clayey sand. At the interface between foundation and dam, the soil is classifiable as silty-clayey sand, whereas, at the depth of 27,50 m soil consists of sand with clayey silt. Clay fraction is about 21% a the top of dams. This value is reduced as the depth increases to a minimum of 12% recorded at 27,7 m.

Table 6. Laboratory tests performed on samples retrieved from borehole

Sample	Tests
C_1 (3.00 ÷ 3.50 m)	Grain size distribution Index properties Oedometer test (OED) Triaxial tests (TX) Resonant column Test (RC) Cyclic Torsional Shear Test (CTS)
C_2 (15.50 ÷ 16.00 m)	Grain size distribution Index properties Oedometer test Triaxial tests Resonant column Test Cyclic Torsional Shear Test
C_3 (27.50 ÷ 28.00 m)	Grain size distribution Index properties Oedometer test Triaxial tests Resonant column Test Cyclic Torsional Shear Test

Table 7. Main physical and state variables of the tested samples

Test	Depth (m)	γ (kN/m³)	γ_d (kN/m³)	e (-)	w_n (%)	Sr (%)
OED	3.20	19.6	15.9	0.688	23.6	93.8
OED	15.50	20.3	17.3	0.560	17.5	85.9
OED	15.60	20.5	17.1	0.580	20.2	95.6
TX-CIU	3.30	19.7	15.9	0.687	23.9	95.1
TX-CIU	3.40	19.7	15.9	0.683	23.8	95.1
TX-CIU	15.70	19.6	16.7	0.612	17.3	77.4
TX-CIU	15.80	20.2	17.3	0.554	16.7	82.6
TX-CIU	27.70	19.6	16.5	0.621	18.7	82.2
RC/CTS	3.10	19.7	15.8	0.700	24.8	97.1
RC/CTS	15.90	20.6	17.6	0.530	17.5	89.9
RC/CTS	27.50	20.6	17.5	0.530	17.8	92.1

OED: Oedometer test; TX-CIU: isotropic consolidated-undrained triaxial test; RC/CTS: resonant column and cyclic torsional shear tests.

According to the Casagrande chart (Fig. 14), the fine portion of shallow samples can be classified as inorganic silt of medium compressibility, while fine portion of the other two deeper samples can be classified as inorganic clays of low plasticity.

The activity chart (Fig. 15) highlights that all of samples are soils with low activity.

Fig. 16 shows the profiles of unit weight (γ), dry unit weigh (γ_d), natural water content (w_n), void ratio (e) and degree of saturation (Sr). It is possible noted that γ is about constant (19.6 ÷20.6) and also water content varies in a small range (16.7÷24.8), and it is close to the Plastic Limit. Degree of saturation (Sr) is between 77.4 and 97.1 %.

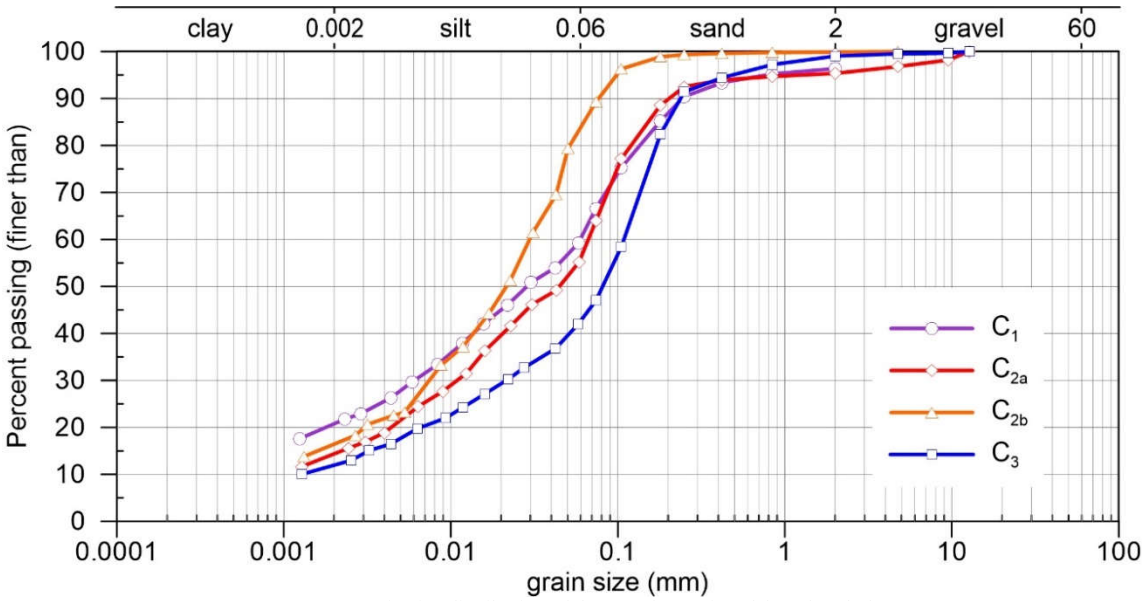

Figure 13. Grain size distribution of the samples retrieved from borehole.

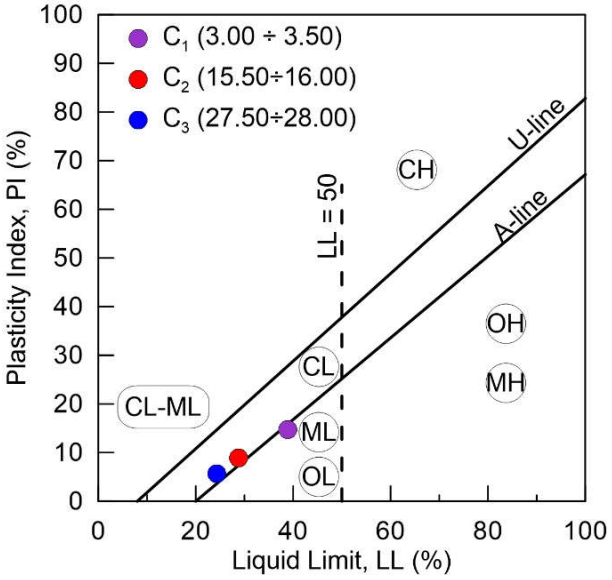

Figure 14. Casagrande chart: classification of samples retrieved from borehole

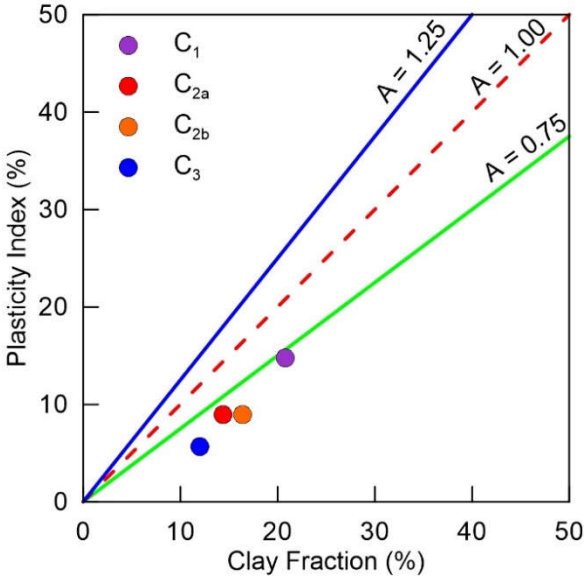

Figure 15. Active chart: classification of samples retrieved from borehole

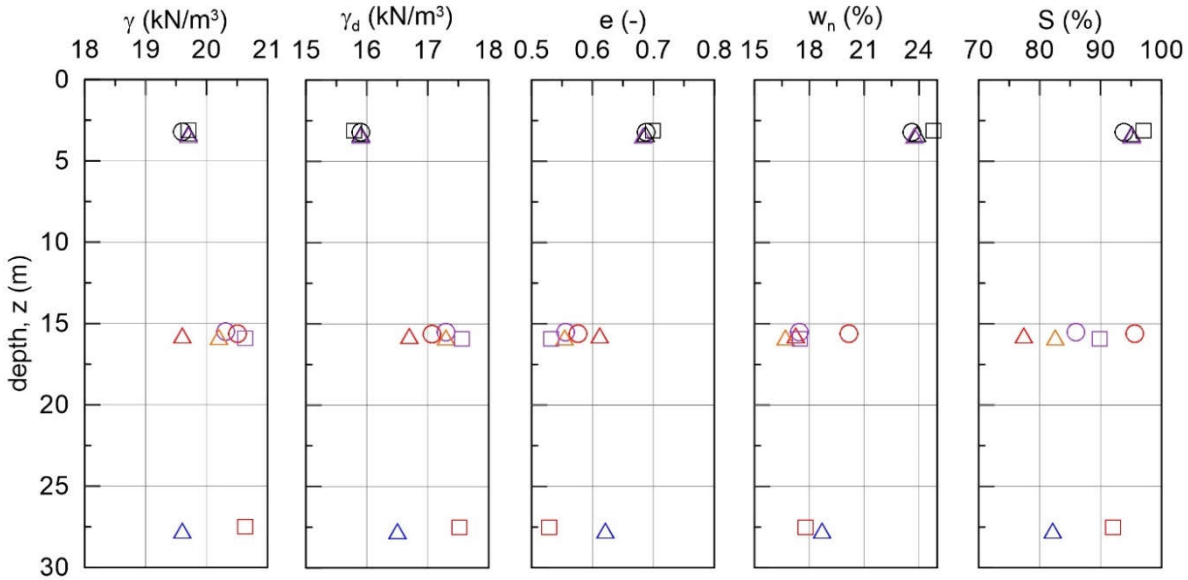

Figure 16. Variation of index and state parameters with depth from the top of dam.

To establish the deformability properties of body of dam and soil foundation, some oedometer tests were performed. Fig. 17 shows compression curves of all tested specimens. It is possible to observe that the shallowest sample is more compressible than deeper ones (Tab. 8), whereas the pre-consolidation stress increases with the depth.

Table 8. Compressibility parameters of samples

Sample	Depth (m)	σ'_p (kPa)	C_R (-)	C_C (-)
C_1	3.20	93	0.04	0.18
C_{2a}	15.50	260	0.04	0.10
C_{2b}	15.60	190	0.06	0.13

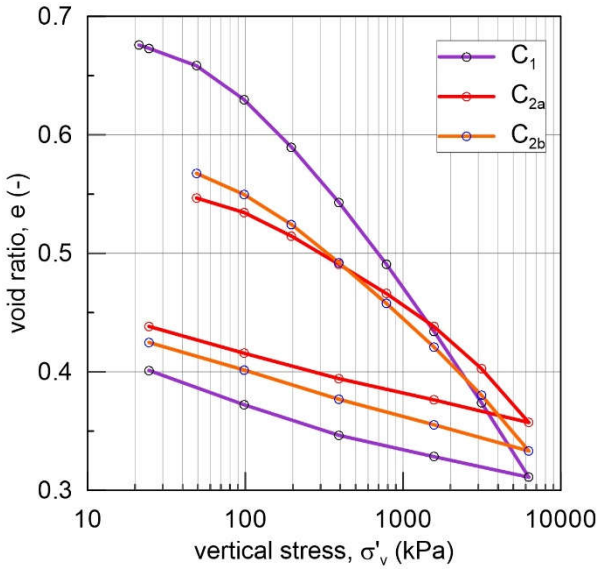

Figure 17. Compression curves.

A set of triaxial tests were performed to evaluate the strength parameters of soils. Specimens were consolidated at the in-situ effective stress or higher pressure (1.5 of the in-situ stress) and then tested in undrained condition. The stress path of each tests are shown in Fig. 18. Figs. 19 and 20 report the results in term of principal stresses ratio versus deviatoric strain and excess pore pressure versus the same strain variable, respectively. Results show a typical softening behavior of over-consolidated soils: principal stresses ratio increases to a peak value and then decreases with increase in strain, in meantime pore water pressure initially increases and then decreases, sometimes becoming negative. Generally, high deformations were applied to reach the critical condition. Two specimens (C_{2a} and C_3) seem far away from the critical state.

A preliminary evaluation of shear strength parameters are reported in Tab. 9.

Table 9. Compressibility parameters of samples

Depth (m)	φ'_{cv} (°)	φ'_p (°)
3.00 ÷ 3.50	32	35
15.50 ÷ 16.00	33	39
27.50 ÷ 28.00	32	33

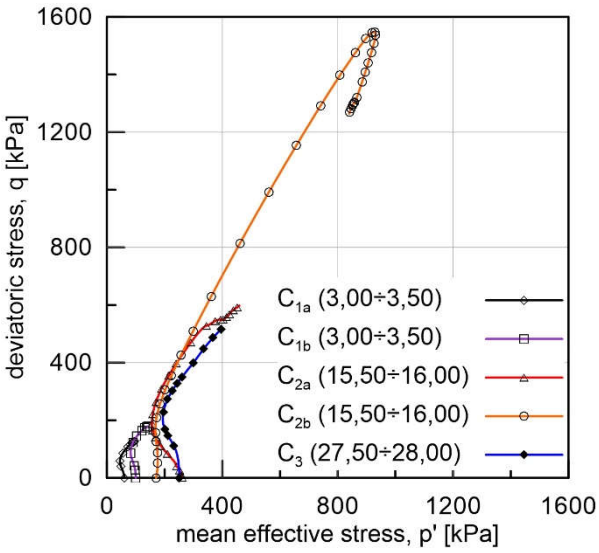

Figure 18. Stress path of triaxial tests.

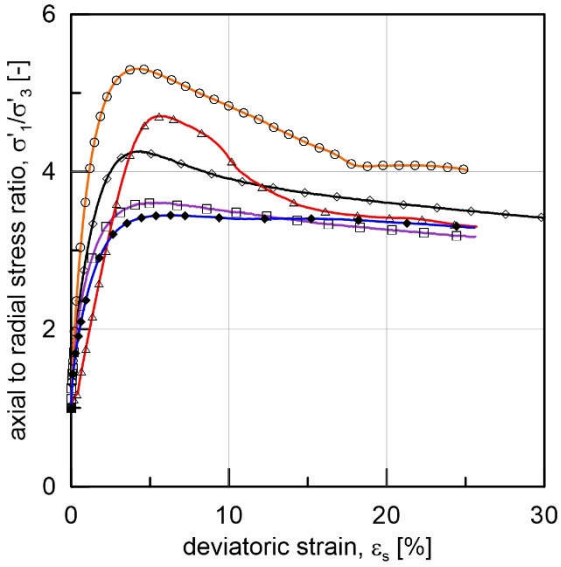

Figure 19. Principal stress ratio versus deviatoric strain diagram.

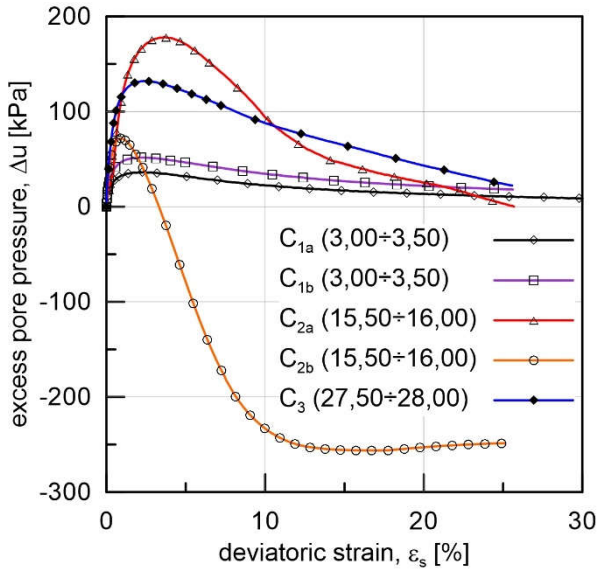

Figure 20. Excess pore pressure versus deviatoric strain diagram.

Deformation properties of dam body and foundation soil were determined through laboratory cyclic tests and dynamic tests (resonant column tests). Three tests were performed on three samples collected at three different depth. Initially, each specimen was isotropically consolidated at the confining pressure corresponding to the sampling depth. Then, the resonant test was performed applying a dynamic torsional oscillation at the top edge of specimen while varying the frequency of the input signal. The response of specimen in term of motion amplitude is measured through an accelerometer so that the fundamental frequency can be found. During the dynamic test the pore pressure is measured through a pressure transducer connected with drainage system. The shear modulus is computed from resonant frequency according the elasticity theory, while the material damping is determined from the free-vibration decay curve observed after stopping the excitation.

The G/G_0-γ and D-γ data points are shown in Figs. 21 and 22, respectively.

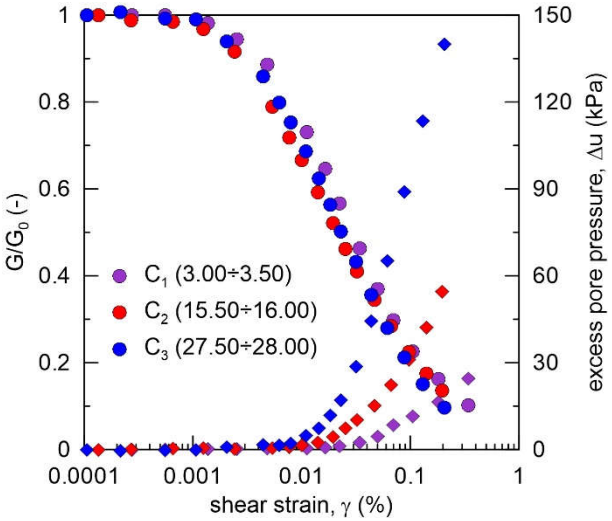

Figure 21. Modulus reduction curves from column resonant test (circular dots) with excess pore pressure evolution (rhomboid dots).

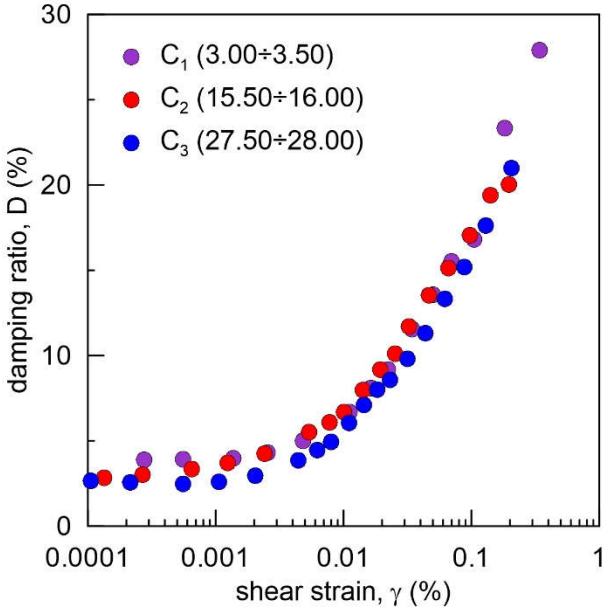

Figure 22. Damping ratio curves from column resonant test.

The plot of excess pore pressure measured during resonant test (Fig. 21) allows the evaluation of volumetric threshold.

Figures highlight the influence of confining pressure and plasticity index on the shear modulus and damping ratio curves. It can be noted that all curves are quite overlapping. This is meanly due to a very narrow range of plasticity index of samples (5.7 ÷ 14.8). Nevertheless, a small effect of confining stress can be observed.

Indeed, it is significant that the sample C_1, characterized by lower confining pressure than other two samples, shows linear cyclic threshold shear strain and volumetric threshold greater than other two curves. In the meantime, the corresponding damping ratio curve is slightly higher than the other two curves.

Finally, cyclic torsional shear tests were performed on same specimens tested with resonant column apparatus. The apparatus is indeed also equipped with two proximity displacement transducers to measure the rotation angle of sample. Using the same electrical motor able to generate a torsional moment is possible to perform a cyclic torsional shear tests. In this case a cyclic torsional moment with very low frequency (0.1 Hz) is applied on the top base of specimen and the corresponding rotation is measured. For each step, 24 loading cycles are applied.

The maximum power of the electrical motor limits the maximum shear strain amplitude that the device is able to measure, therefore it depends on the stiffness of sample. During all phases of test, pore pressure can be measured through a pressure transducer connected with drainage system.

Figs. 23 show an example of results in terms of stress-strain cyclic obtained from the test performed on the specimen C_1 (3.00÷3.50).

It is possible to observe how increasing the level of stress, the stress-strain loops increase their inclination and become larger.

Fig. 24 shows typical cyclic degradation phenomenon due to the pore pressure generation and structural changes that cause the shear strain amplitude of the soil specimen to increase with increasing numbers of cycles.

Figs. 25 and 26 show a comparison between the G/G_0-γ and D-γ data points obtained from column resonant tests and from cyclic torsional shear test.

It is possible to observe that the reduction modulus curves obtained from the cyclic torsional shear test (CTS) are generally located slightly above the respective ones obtained from column resonant test.

In term of damping ratio curve, the CTS results lie below the respective curves obtained from column resonant tests.

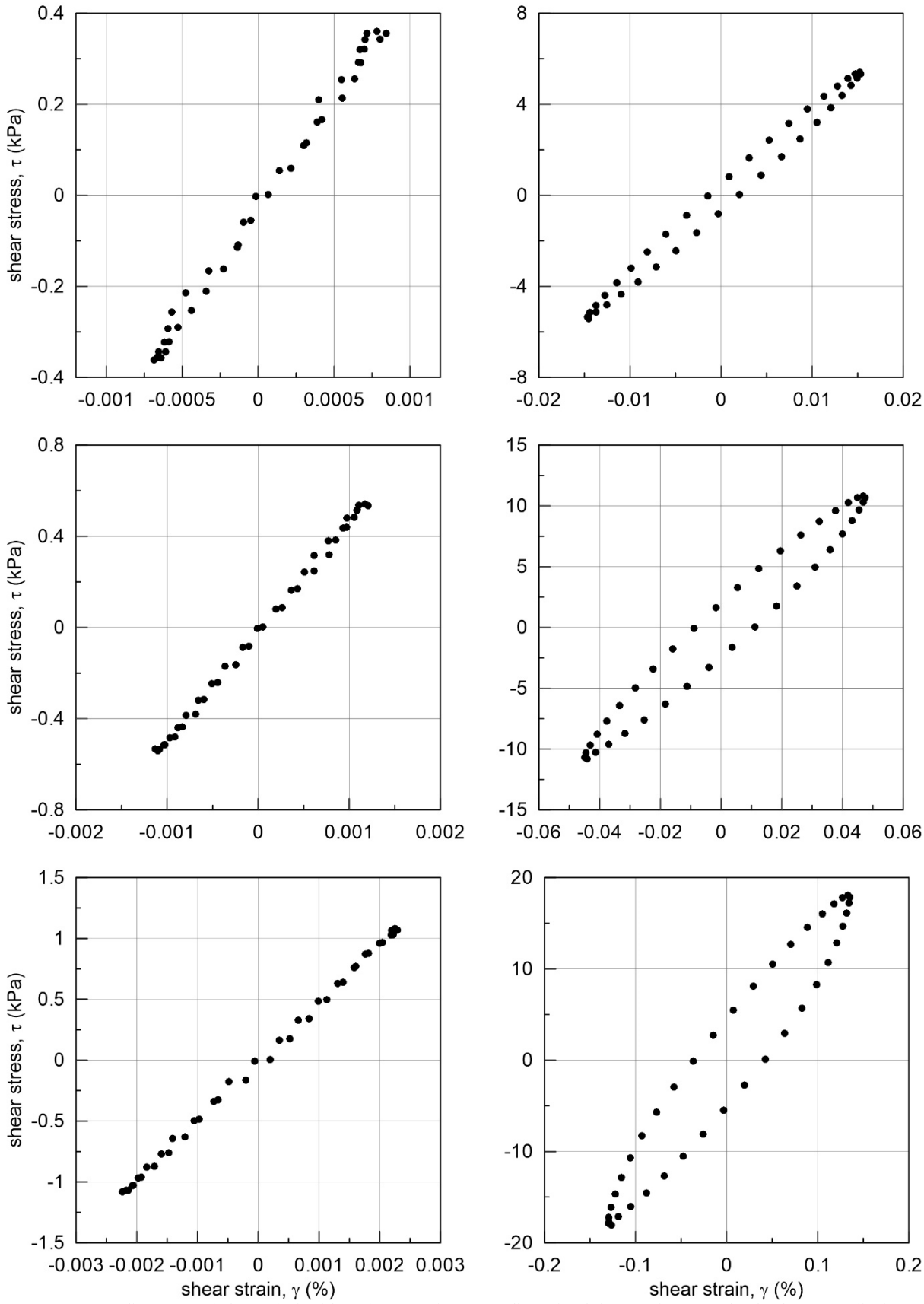

Figure 23. Cyclic stress-strain loops obtained from the C_1 specimen in cyclic torsional shear test increasing levels of stress amplitude.

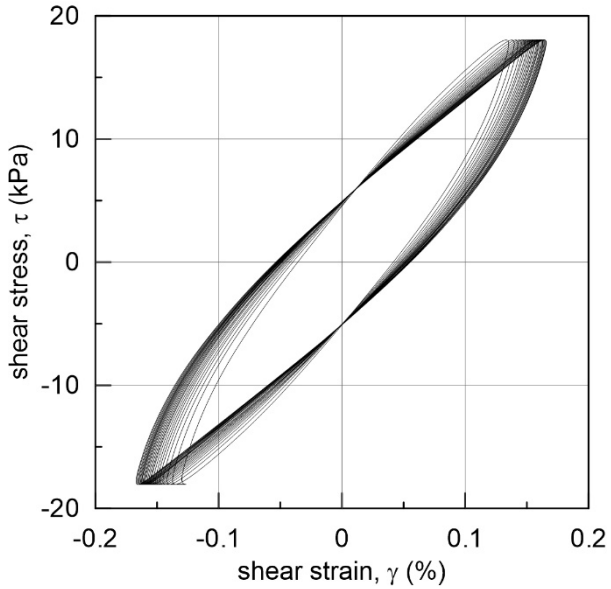

Figure 24. Effect of cyclic degradation on stress-strain loops.

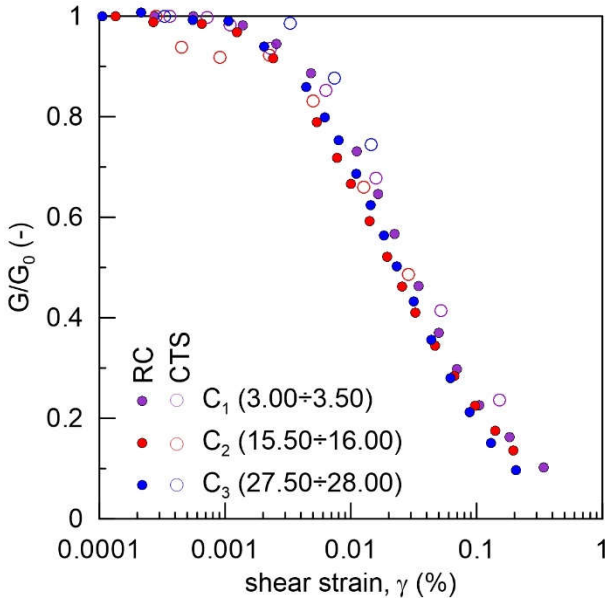

Figure 25. Modulus reduction curves from column resonant test and cyclic torsional shear test.

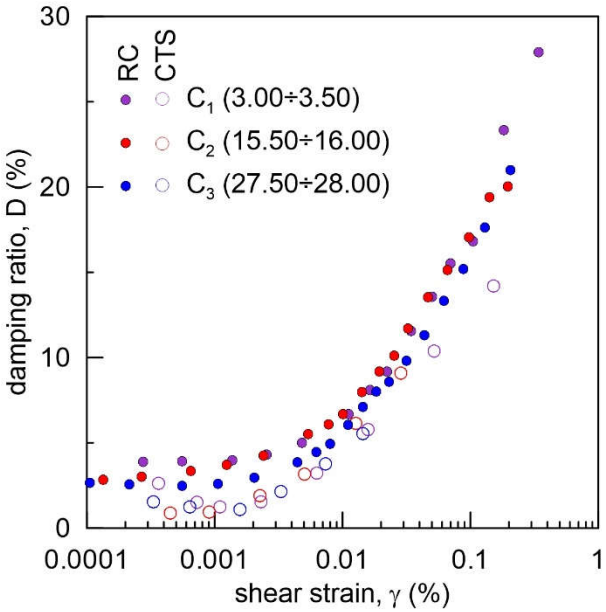

Figure 26. Damping ratio curves from column resonant test and cyclic torsional shear test.

4. Numerical model

The gathered experimental results and the geometrical data allowed us to define a complete numerical model of the dam located within the municipality of Briaglia (CN), Italy. Fig. 27 shows the mesh of the finite difference model.

The main parameters adopted for each layer are reported in Tab. 10.

Table 10. Main parameters of numerical model

Layer	Depth (m)	V_S (m/s^2)	φ' (°)
Dam 1	0.00 ÷ 4.50	160	32
Dam 2	4.50 ÷ 5.80	190	32
Dam 3	5.80 ÷ 7.60	230	38
Dam 4	7.60 ÷ 14.00	270	35
Foundation 1	14.00 ÷ 20.00	500	38
Foundation 2	20.00 ÷ 30.00	800	34
Bedrock	30.00 ÷ 32.00	1500	-

The experimental modulus reduction and damping ratio curve are also assigned to each layers.

Dynamic analyses will be performed by using finite difference commercial software FLAC®. In this respect a set of about 10 real accelerograms recorded at rock outcropping sites for the return period of 475 years will be selected on the basis of French-Italy Alps seismic hazard.

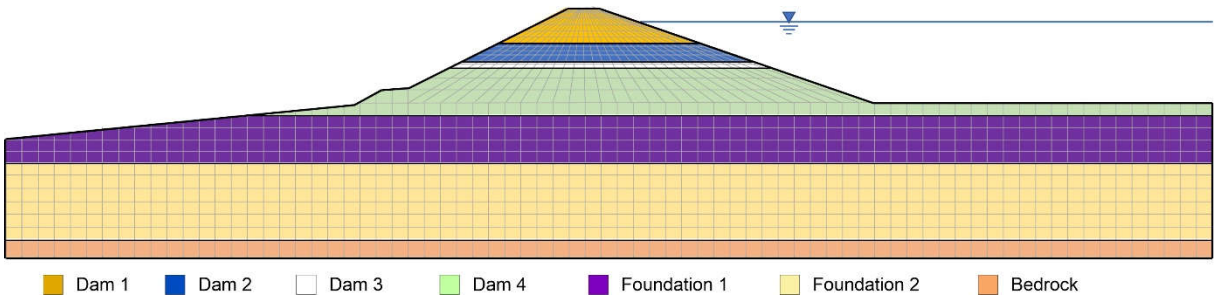

Figure 27. Numerical model of dam located within municipality of Briaglia (CN), Italy.

5. Conclusions

Advanced seismic risk analyses of earth dams require an in-depth knowledge of the structure in terms of stratigraphy of dam body and foundation soil, physical and mechanical properties of soils. These type of analyses can be typically performed only for "large" dams where technical information and a great number of data are available. Instead "small" dams are often characterized by lack of technical information and simpler methods are needed to assess the seismic risk.

However, the risk associated with the potential rupture of these last type of dams can be considerable, since they are often located along slope close to populated areas. An increase of their knowledge allows for the adoption of advanced method of analysis and hence consecutively the resilience of the community.

In this respect an extensive characterization campaign has been performed on some small earth dams located in the French-Italian Alps.

Different in-situ geotechnical tests have been performed: boreholes, seismic piezocone penetration tests (SCPTU), and flat dilatometer tests (DMT). Several laboratory tests have been also carried out on samples retrieved from boreholes: Oedometer tests (OED), Consolidated-Undrained Triaxial tests (TX-CIU), Column Resonant Tests (CR), and Cyclic Torsional Shear tests (CTS). Finally, invasive and non-invasive geophysics tests have been conducted: Multi-channel Analysis of Surface Waves (MASW), Ambient Vibration Survey (AVA), Horizontal to Vertical Spectral Ratio (HVSR), Electric Resistivity Tomography (ERT), and Down-hole tests (DH).

The results of tests performed on the dams located within the municipality of Briaglia (CN), Italy have been discussed in detail in the present paper.

The gathered experimental results allowed the definition of a complete numerical model on which advanced dynamic analyses can be performed.

A comparison of the results of these numerical analyses with simplified pseudo-empirical methods could provide a general framework and guidelines for establishing a rapid assessment of the seismic risk of small earth dams of French-Italy alpine regions.

Acknowledgement

The project presented in this article is supported by the European Union for regional development (Interreg-ALCOTRA) for the French-Italy Alps, within the "ReSba" (Resilienza degli Sbarramenti) project. The Authors are grateful to R. Del Vesco, D. Patrocco, G. Bodrato and S. La Monica from Piedmont Region Administration for their availability and support. Thanks to C. Etna and F. Damiano, two master students who worked actively in the first part of this study, and A. Ciancimino for helping with the interpretation down-hole tests. Special thanks to G. Bianchi, technician of Geotechnical Laboratory at Politecnico di Torino for the laboratory tests.

References

[1] Ministero delle Infrastrutture e Trasporti, Decreto 26/06/2014. Gazzetta Ufficiale Serie Gen. N. 156 del 08/07/2014, Norme Tecniche per la Progettazione e la Costruzione degli Sbarramenti di Ritenuta (dighe e traverse)..

[2] Ministero delle infrastrutture e Trasporti, Decreto 17/01/2018. Gazzetta Ufficiale Serie Gen. N. 42 del 20/02/2018, Aggiornamento delle «Norme tecniche per le costruzioni».

[3] Lanzo, G., "Alcune considerazioni sulla rivalutazione della sicurezza sismica delle dighe di materiali sciolti ", In: Fot. S, Cosentini R.M., Dominijianni A. (eds.) Analisi e progetto delle opera geotecniche in zona sismica, Politecnico di Torino, Torino, Italy, 2018, pp. 1–44.

[4] Russo, C., Costigliola R., Pagano, L. and Silvestri, F. "Dighe in terra: meccanismi di danneggiamento e Stati Limiti in condizioni sismiche". In XXVI Convegno Nazionale di Geotecnica "La Geotecnica nella Conservazione e Tutela del Patrimonio Costruito", Roma, Italy, 2017, vol. 1, 323-333.

[5] ISPRA, "Stato dell'ambiente 84/2019", Roma, Available at: http://www.isprambiente.gov.it/it/pubblicazioni/stato-dellambiente/annuario-dei-dati-ambientali-edizione-2018.

[6] Cosentini R.M., Passeri F., Foti S. "A simplified methodology for the assessment of the seismic risk associated with small earth dams", In F. Calvetti et al. (Eds.), Geotechnical Research for Land Protection and Development, Proceedings of CNRIG, Springer Nature AG, Switzerland, 2020 pp. 93-100. https://doi.org/10.1007/978-3-030-21359-6_10

[7] Regione Piemonte "Regolamento regionale di attuazione della legge regionale 6 ottobre 2003, n. 25 (Norme in materia di sbarramenti fluviali di ritenuta e bacini di accumulo idrico di competenza regionale. Abrogazione delle leggi regionali 11 aprile 1995, n. 58 e 24 luglio 1996, n. 49). B.U. 11/11/2004 n. 45

[8] Swaisgood, J. R. "Embankment dam deformations caused by earthquakes", In: 7th Pacific Conference on Earthquake Engineering, Christchurch, New Zealand, 2003

[9] Blake, T., Hollingsworth, R. and Stewart, J. "Recommended procedures for implementation of DMG. Special Publication 117 guidelines for analyzing and mitigating landslide hazards in California", ASCE Los Angeles Section Geotechnical Group. California Geological Survey, 2002.

[10] Foti, S., Hollender, F., Garofalo, F. et al. "Guidelines for the good practice of surface wave analysis: a product of the InterPACIFIC project", Bulletin Earthquake Engineering, 16(6), pp. 2367-2420, 2018. https://doi.org/10.1007/s10518-017-0206-7

[11] Socco, L.V., Boiero, D., "Improved Monte Carlo inversion of surface wave data", Geophysical Prospecting, 56(3), pp. 357-371, 2008. https://doi.org/10.1111/j.1365-2478.2007.00678.x

[12] Sesame Team. "The SESAME project: an overview and main results", In: 13th World Conf. on Earthquake Engineering, Vancouver, BC, Canada, 2004, pp. 1-6.